Available online at www.sciencedirect.com
SCIENCE DIRECT®
Journal of Computational Physics 189 (2003) 512–526
JOURNAL OF COMPUTATIONAL PHYSICS
www.elsevier.com/locate/jcp

Statistical simulation of rarefied gas flows in micro-channels

Ching Shen *, Jing Fan, Chong Xie

Laboratory for High-Temperature Gas Dynamics, Institute of Mechanics, Chinese Academy of Sciences, Beijing 100080, China

Received 8 July 2002; received in revised form 4 April 2003; accepted 11 April 2003

Abstract

Rarefied gas flows through micro-channels are simulated using particle approaches, named as the information preservation (IP) method and the direct simulation Monte Carlo (DSMC) method. In simulating the low speed flows in long micro-channels the DSMC method encounters the problem of large sample size demand and the difficulty of regulating boundary conditions at the inlet and outlet. Some important computational issues in the calculation of long micro-channel flows by using the IP method, such as the use the conservative form of the mass conservation equation to guarantee the adjustment of the inlet and outlet boundary conditions and the super-relaxation scheme to accelerate the convergence process, are addressed. Stream-wise pressure distributions and mass fluxes through micro-channels given by the IP method agree well with experimental data measured in long micro-channels by Pong et al. (with a height to length ratio of 1.2:3000), Shih et al. (1.2:4800), Arkilic et al. and Arkilic (1.3:7500), respectively. The famous Knudsen minimum of normalized mass flux is observed in IP and DSMC calculations of a short micro-channel over the entire flow regime from continuum to free molecular, whereas the slip Navier–Stokes solution fails to predict it.

PACS: 85.85.+j; 47.45.−n; 02.70.Ns

Keywords: Rarefied gas flow; Long micro-channels; MEMS; DSMC method; IP method; Conservative form of mass conservation equation; Super-relaxation method

1. Introduction

As a basic element of MEMS devices, micro-channel gas flows have been studied experimentally and theoretically. In the experiments [1–7], the typical channel dimensions were about 1 μm high by several tens of microns wide and by several thousands of microns long. The flow was driven by the pressure difference between the inlet and outlet that led to a typical inlet velocity of about 0.2 m/s [8]. It was observed that the stream-wise pressure profiles were non-linear, while the measured mass flux was higher than the Navier–Stokes solution based on non-slip boundary condition [1–7]. To take into account this non-continuum

* Corresponding author. Tel.: +86-10-62623973; fax: +86-10-62561284.
E-mail address: cshen@imech.ac.cn (C. Shen).

0021-9991/$ - see front matter
doi:10.1016/S0021-9991(03)00231-6

effect, a velocity-slip boundary condition was introduced analytically or numerically in solving the Navier–Stokes equation [2,9]. Properly choosing the tangential momentum accommodation coefficient (TMAC) σ_t, the slip Navier–Stokes solution agreed with the measured data when the Knudsen number, $Kn = \lambda/h$, is smaller than 0.1, where λ is the molecular mean free path, and h is the channel height [6,7,9]. Kinetic theory indicates that all continuum models break down at a sufficiently high Kn. This was also verified by further micro-channel experiment: the slope of the Navier–Stokes flow conductance obviously deviated from the experimental data at an outlet Knudsen number of about 1.95 [7].

The focus of the present work is to provide a kinetic description of micro-channel gas flows at different experimental conditions [1,5–7]. Because of a small characteristic velocity of 0.2 m/s, conventional kinetic schemes such as the direct simulation Monte Carlo (DSMC) method face a serious statistical noise arising from the thermal velocity. It requires a sample size of 10^8 to isolate the flow velocity of 0.2 m/s from the noise. The boundary conditions at the inlet and the outlet of the long channel need to be adjusted gradually in the simulation, which makes the converging process of the DSMC simulation extremely time-consuming. The computational demand in the huge sample size and extremely large time consumption of the DSMC made it beyond the current computer capabilities [10]. The authors proposed a particle-based method, called the information preservation (IP) method [11,12], which was proven highly effective to reduce the statistical noise, for instance, a sample size of 10^4 is enough for IP to resolve a macroscopic velocity of 0.2 m/s in the background of room temperature gas, four orders less than that required by DSMC. The IP method has been successfully applied to benchmark problems, namely Couette flow, Poiseuille flow and Rayleigh flow, over the entire Knudsen regime [11,12]. The macroscopic velocity, surface shear stresses and mass fluxes given by IP were in excellent agreement with exact solutions in the continuum and free molecular regimes, and with experimental data [13] and the linearized Boltzmann solutions [14,15] in the transition regime. Recently, Sun et al. [16] simulated low subsonic air flows past a flat plate of 20 μm long over the entire Knudsen regime using IP. The drag coefficient given by IP compared well with experimental data of Schaff and Sherman [17] and Janour [18].

Application of the IP method to micro-channel flows is straightforward and has been demonstrated in preliminary studies [19,20]. For a micro-channel of 1.2 μm high by 3000 μm long, with the inlet and outlet pressures of 20 and 0 psig, respectively, the stream-wise pressure distribution obtained by IP agreed well with the experimental data of Pong et al. [1]. Specific complications naturally arose. In solving the low speed micro-channel flow problem as any micro-scale low speed internal flow problem there arose the issue of mutual interaction of the inlet and outlet boundary conditions caused by the elliptical nature of the problem. This issue becomes serious for large length to height ratio of the channel where a long regulating process to adjust the mass flux to be the same at any cross-section is needed. And the available experimental data are namely for long aspect ratio 3000 (or 4000) to 1.2 [1,5] and 7500–1.3 [6]. In this paper, we shall simulate micro-channel gas flows over the entire flow regime and compare the results with measured data available. Firstly, certain issues in IP calculation are addressed. The suggestion to use the conservative form of the mass conservation equation for IP values to guarantee the adjustment of the mass flux and the super-relaxation scheme to accelerate the convergence process and its necessity is illustrated. Then the tangential momentum accommodation coefficient along micro-channel surfaces in experiment is discussed. Next, the IP method is used to simulate micro-channel gas flows at various experimental conditions. In addition, both IP and DSMC calculations are made for a short micro-channel over the entire Knudsen regime. Finally, some conclusions are given.

2. Computational issues

In the IP method, a relatively small number of model molecules is stored in a computer to represent the large number of molecules in real gas flows and each simulated molecule is assigned two velocities: thermal

velocity $\vec{c}_i$ and information velocity $\vec{u}_i$ [11,12]. A simulated molecule moves through physical space and undergoes collisions appropriate to the thermal velocity, following the same algorithms and models as the DSMC method [21], while the information velocity corresponds to the collective velocity of the enormous number of real molecules represented by the simulated molecule. Implementation of the IP method for multi-dimensional flows has been described in detail [20,22–24], and may be briefly summarized as follows:

1. Initially, $\vec{u}_i$ is set based on an initial velocity field.

2. For simulated molecules diffusely reflected from a wall, $\vec{u}_i$ has the same velocity as the wall. If the wall has a TMAC of value σ_t the reflected molecule with a probability of σ_t has an IP velocity the same as the wall, and with a probability $(1-\sigma_t)$ retains its tangential velocity before incidence.

3. For simulated molecules entering the computational domain from boundaries, $\vec{u}_i$ is set to satisfy the boundary condition.

4. For two simulated molecules colliding each other, the post-collision velocities satisfy the momentum conservation

$$u_{i,1}^* = u_{i,2}^* = \frac{m_1 u_{i,1} + m_2 u_{i,2}}{m_1 + m_2}, \tag{1}$$

where superscript * denotes post-collision.

5. If there are external forces acting on a cell, acceleration $\vec{a} = \vec{F}/\rho\Delta V$ will contribute an velocity increment $\vec{a}\Delta t$ to each simulated molecule during a time step Δt, where $\vec{F}$ is the sum of the external forces, ρ and ΔV are the density and volume of the cell, respectively.

6. The shear stress on a surface element with area ΔA_w is given by

$$\tau_w = \frac{\sum_{j=1}^{N} m(u_{\tau,j}^{\mathrm{in}} - u_{\tau,j}^{\mathrm{re}})}{t_s \Delta A_w}, \tag{2}$$

where N is the total number of molecules hitting the element during the sampling interval t_s, subscript τ denotes the tangential direction of the element, and superscripts in and re denote the incident and reflecting values, respectively.

7. In general under the isothermal assumption (which is valid for slow subsonic channel flows without heating) the IP velocity $\vec{u}_i$ of the simulated molecule and the IP velocity $\vec{U}$ and IP density ρ (or n) of the cell are introduced which obey the mass conservation and momentum conservation equations

$$\int\int\int \frac{\partial \rho}{\partial t}\,\mathrm{d}V = \int\int \rho \vec{U}\cdot\vec{l}\,\mathrm{d}S, \tag{3}$$

$$\int\int\int \rho \frac{\mathrm{d}\vec{U}}{\mathrm{d}t}\,\mathrm{d}V = -\int\int p\vec{l}\,\mathrm{d}S, \tag{4}$$

where the integrals are taken on the volume and surfaces of a cell, $\vec{l}$ is the external normal vector of the surface. It is noted that in the right-hand side of the momentum equation only a non-viscous term is retained. In fact the IP quantities are governed by a general momentum equation

$$\int\int\int \rho \frac{\mathrm{d}\vec{U}}{\mathrm{d}t}\,\mathrm{d}V = -\int\int \vec{\vec{\sigma}}\vec{l}\,\mathrm{d}S \equiv -\int\int p\vec{l}\,\mathrm{d}S + \int\int \vec{\vec{\tau}}\vec{l}\,\mathrm{d}S, \tag{5}$$

where $\vec{\vec{\sigma}}$ is the pressure stress tensor and $\vec{\vec{\tau}}$ is the viscous stress tensor. But as the IP quantities are carried along by the simulated molecules of the DSMC process which migrate across the cell surface in the positive and negative direction and implement the action of viscous transport, so the IP quantities are factually governed by the equation with only the normal stress acting on the surface retained. After a time step Δt the cell IP density and velocity attain increments according to (3) and (4)

$$\Delta\rho = -\frac{\Delta t}{\Delta V}\int\int \rho\vec{U}\cdot\vec{l}\,\mathrm{d}S, \tag{6}$$

$$\Delta\vec{u} = -\frac{\Delta t}{\rho\Delta V}\int\int p\vec{l}\,\mathrm{d}S, \tag{7}$$

and are added to the IP density and velocity of the simulated molecules in the cell. The cell pressure is also renewed: $p = nkT$. The renewed quantities are used for the next step calculation.

In the following some specific computational issues encountered in simulating low speed flows in long micro-channels by using the IP method is addressed.

The geometric form of the micro-channel flow is quite simple (see Fig. 1), but it is able to reveal the distinguishing feature of the low speed micro-scale internal flow, i.e., the issue of the mutual influence of the inlet and outlet boundary conditions caused by the elliptic nature of the problem. For the DSMC-IP procedure it is necessary to prescribe the values of the pressure p and the velocity distribution $\vec{U}$ over the cross-sections at the inlet and the outlet of the channel to start any simulation. But fixing all p and $\vec{U}$ at the inlet and the outlet simultaneously would over determine the boundary conditions: The arbitrarily chosen p and $\vec{U}$ would be contradictory to each other. The correct values of p and $\vec{U}$ at inlet and outlet must be obtained in the process of solution of the problem. A method of fixing p as the same of the experimental condition and allowing $\vec{U}$ to change continuously and finally reach the steady solution is adopted here [20]. Thus the process of the DSMC-IP solution is always one of gradual adjustment towards a steady state: The flow field with different mass fluxes at various cross-sections of the channel is gradually adjusted to a flow field with the same mass flux everywhere. It is very critical that the conservative form of the mass conservation equation must be employed,

$$\frac{\partial\rho}{\partial t} + \frac{\partial\rho U}{\partial x} + \frac{\partial\rho V}{\partial y} = 0, \tag{8}$$

its second-order central difference scheme yields the density increment

$$\Delta\rho = \Delta t\left(\frac{\rho_{i-1,j}U_{i-1,j} - \rho_{i+1,j}U_{i+1,j}}{2\Delta x} + \frac{\rho_{i,j-1}V_{i,j-1} - \rho_{i,j+1}V_{i,j+1}}{2\Delta y}\right). \tag{9}$$

This density increment expression can be obtained from the integral form mass conservation equation (6) directly by using an integration domain ABCD ($2\Delta x \times 2\Delta y$) with point (i, j) in the center (see Fig. 2). The adoption of the conservative form of the continuum equation or the integral form of conservation equation guarantees that the mass flux flown from the adjacent domain of area ABCD will flow without any numerical error into the integral area and vice versa and avoids the accumulation of numerical errors from the non-conservative scheme. This is an issue that must be taken into account whenever solving a slow rarefied channel flow or any other slow internal rarefied gas flows.

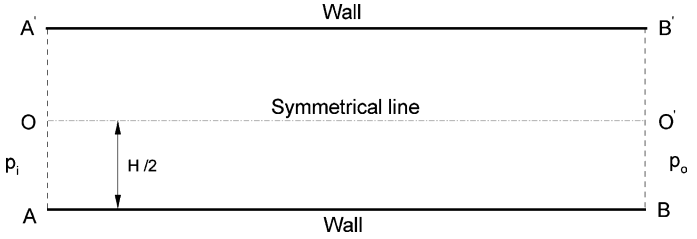

Fig. 1. Computational domain of a micro-channel gas flow.

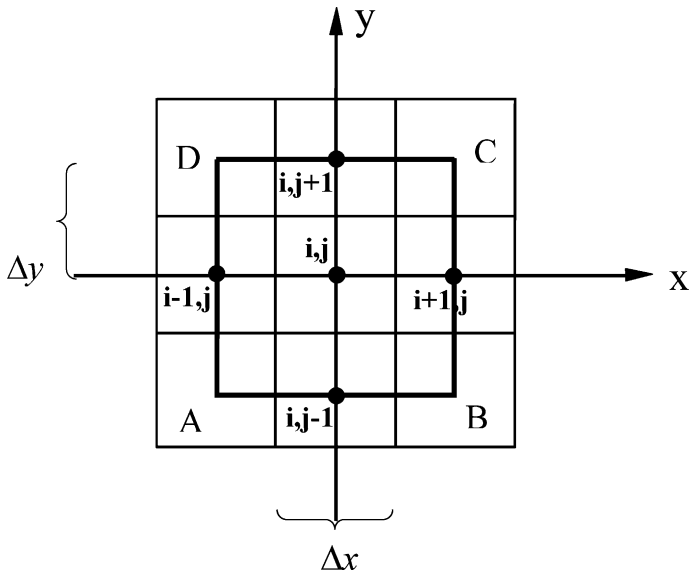

Fig. 2. The control surface ABCD of the conservation equation and the cell central points (i, j) in the IP method, for the derivation of (9).

The increments $\Delta\rho$ and Δu from (9) and (7) allow one to obtain the renewed fields of ρu and ρv which are unfortunately with large fluctuations and are smoothened by a averaging technique to avoid the amplification of the errors which would influence the stability of the calculation. The increment $\Delta\rho$ obtained from (9) is only of the order of 10^{-9} of ρ with time step Δt being of the collision time for slow gas motion in long micro-channels [1,5,6]. For all simulations in such channel flows Δt has been taken as 1/2 average collision time at the inlet. Direct employment of this $\Delta\rho$ to achieve the steady (convergent) state is too time-consuming. A super-relaxation technique is employed to speed up the convergence process

$$\rho_{i,j}^{t+\Delta t} = \rho_{i,j}^{t} + \omega\Delta\rho_{i,j}^{t}, \tag{10}$$

where ω is the relaxation factor. In practical calculations ω is taken to be between 100 and 2000 and tends to 1 when convergence is achieved. [1]

The necessity of using the conservative form of the mass conservation is illustrated on one of the flow cases under the experimental conditions considered [5]. Helium flows through a $1.2 \times 40 \times 4000\ \mu m^3$ micro-channel with an inlet pressure of 19.0 psig into the atmosphere (outlet pressure 0 psig). Figs. 3 and 4 show the evolution of mass fluxes at all cross-sections along the channel by the IP calculation. The slip Navier–Stokes solution is adopted as the initial pressure distribution. It is different from the real distribution since the flow is in the transitional regime. This results in a non-uniform mass flux distribution along the channel length at the initial stage of simulation (at $1\sim2 \times 10^3\ \Delta t$, the black triangles in Figs. 3 and 4). By using the conservative scheme (9) and the super-relaxation technique (10) a steady state is approached after about 2×10^5 time steps (the hollow spheres in Fig. 3). And the averaging-smoothing process gives a relatively smooth and almost uniform mass flux distribution (solid line in Fig. 3). If the non-conservative scheme were used the mass flux would remain non-uniform. Fig. 4 shows the mass flux distribution after 2×10^5 time

[1] For short channels and not slow flow speed, $\Delta\rho_{i,j}^{t}$ might be the same order of $\rho_{i,j}^{t}$, and an ω less than 1 is suggested to be used to stabilize the convergence process.

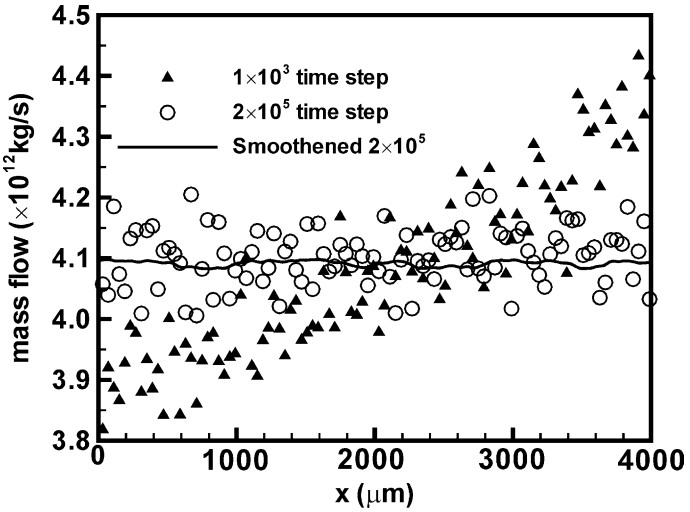

Fig. 3. Evolution of mass flux distribution in IP simulation of a micro-channel gas flow under experimental conditions of Shih et al. [5] while the conservative form of the mass conservation equation is used.

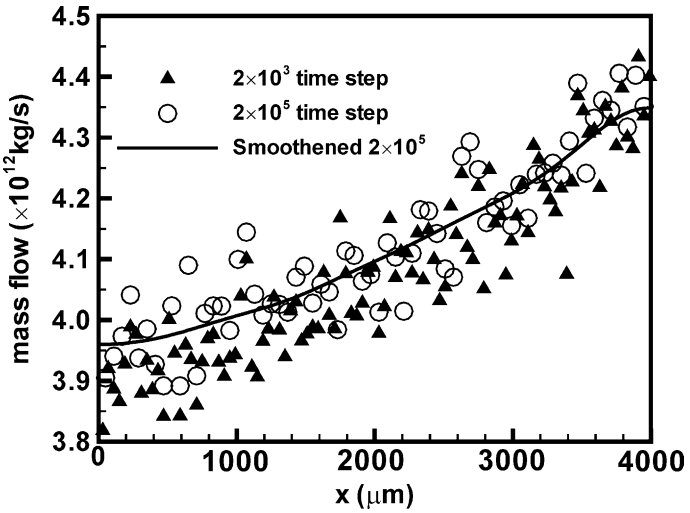

Fig. 4. Evolution of mass flux distribution in IP simulation of a micro-channel gas flow under experimental conditions of Shih et al. [5] while a non-conservative form of the mass conservation equation is used.

steps (the hollow spheres, the solid line being the averaged smoothened data) by using the non-conservative form of the continuity equation. The mass fluxes at various cross-sections have not been regulated by the simulation relaxation process, for the adjusting act of the mutual influence of the inlet and outlet boundaries have been damped by the numerical errors inherent in the non-conservative scheme.

The effect of the acceleration action of the super-relaxation technique is illustrated on another experimental case [1] of nitrogen flowing in a $1.2 \times 30 \times 3000\ \mu m^3$ channel with inlet pressure of 15 psig into the atmosphere. Fig. 5 shows the evolution of the density ρ at the center of the cross-section located at 2500 μm from the inlet in the IP calculation by using a super-relaxation factor ω of 1, 100 and 1000,

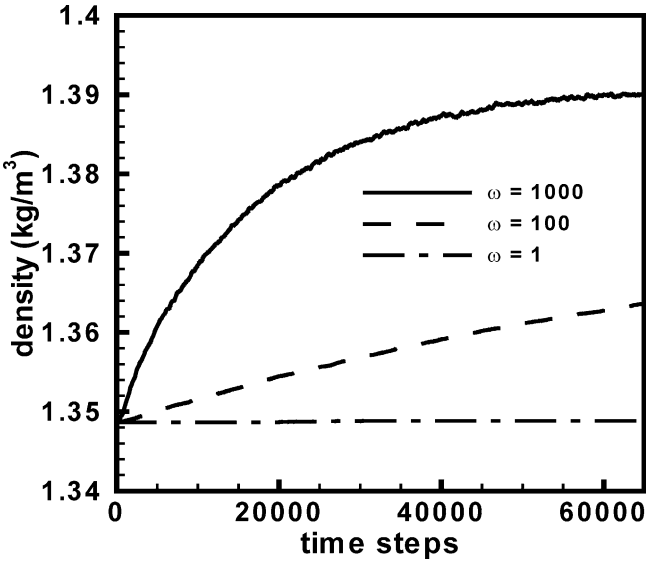

Fig. 5. The evolution processes of density ρ at a point located at 2500 μm apart from the inlet under experimental conditions of Pong et al. [1] with different super-relaxation factors $\omega = 1$, $\omega = 100$ and $\omega = 1000$, respectively.

respectively. While ρ approaches the steady value of 1.39 kg/m^3 in about 6×10^4 time steps with a relaxation factor ω of 1000, the evolution for $\omega = 100$ is further than halfway apart from the steady state after 6×10^4 time steps, and the value of ρ remains almost the same when no super-relaxation is employed (with $\omega = 1$). The maximum value of ω allowed in simulation is dependent on the smoothing technique of mass fluxes in the whole flow field: the smoother the mass flux, the larger value ω is allowed. But exaggerated smoothing would distort the flow field. A simple averaging from adjacent three points, $M(i,j,n) = (M(i-1,j,n-1) + M(i,j,n-1) + M(i+1,j,n-1))/3$, where n is the number of iterations, is used. The iterated averaging for $n = 15$ has the desirable effect of smoothing and retains the local trend of mass flux evolution. Then the value $\omega = 2000$ can be employed and the calculation remains stable. It is noted that when the steady value of ρ is being approached the value of ω and the smoothing procedure has little consequence on the final evolution result, so after having experience one can prescribe ω a varying process from say 2000 to 1 to reach the steady state, and the final result is entirely not effected by the varying process. This is satisfactory for the purpose of the calculation, for it is the final result but not the evolution process that is concerned.

In the practice of general IP method the DSMC simulated molecules move and carry the IP quantities, the DSMC process determines the IP process and the IP process has no reverse influence on the DSMC process. In the solution of channel flow and other internal flow cases, where the macroscopic quantities on the boundaries are to be regulated during the simulation, there is another specific feature, that is, the varying IP velocities on the boundaries are used to continuously adjust the boundary conditions of the DSMC–IP procedure. This influences the DSMC simulation and enables the DSMC finally to have the correct value on the boundaries. Pure DSMC process is carried out by individual molecules and the adjustment of boundary conditions is very slow and DSMC needs sufficient sample size to allow definite boundary values of $\vec{U}$ to emerge, while the IP process is a global one: the changes of IP values happened simultaneously over the whole domain of calculation and with the help of super relaxation the adjustment is quick and not limited to the boundary but spreads over all the channel length. Although the approach to the steady state requires quite a long time in the example calculation under the experimental

condition [1] (120 h CPU time on a Pentium III 450, or 98.7% of the entire computation time), but during this time the global DSMC quantities are also regulated. After arriving at the steady state the sampling time required for yielding the final IP convergent data is quite short (1.6 h CPU time, or 1.3% of the computation time).

3. Computational conditions

In micro-channel experiments performed by Pong et al. [1], Shih et al. [5], Arkilic et al. [6] and Arkilic [7], respectively, the channel width is much larger than the height (Table 1). This made the span-wise influence negligible, and the flows can be simplified as two-dimensional (the midline velocity profile and the maximum velocity remains the same for rectangular cross-section channels with a width to height ratio larger than 5, but the flow rate is influenced in some minor degree by the slow down of the flow near the side wall even for large width to height ratio). The degree of rarefaction is measured by the Knudsen number with the channel height as the characteristic length. The Knudsen number at the outlet, Kn_o, indicates that the experimental conditions [1,5–7] are in the slip and transition regimes, respectively.

An orthogonal coordinate system is employed here, with the origin at point O, and x and y axes along OO′ and OA, respectively (see Fig. 1). Since the flows are symmetric about OO′, we consider a computational domain of OO′BA that is divided into uniform rectangular cells. Each of the cells is sub-divided into a set of uniform rectangular sub-cells within which collision pairs are selected. The numbers of cells and sub-cells in each cell are given in Table 1. The cell size is much smaller in the normal direction than in the stream-wise direction, so is the sub-cell size. As shown by Nance et al. [25], the flow field is insensitive to the stream-wise cell size because of a relatively small velocity gradient in this direction. Our test calculations also verify this observation that the smaller stream-wise cell and sub-cell sizes provide the same results as the present ones. For all cases the molecular interaction is described by using the variable hard-sphere (VHS) model [21]. The VHS model assumes that the scattering from molecular collision is isotropic in the center of mass frame of reference, whereas the collision diameter depends on the relative velocity. The reference collision diameter in VHS appropriate to the IP method has been determined for common gases [12].

A specular reflection is used along the symmetrical boundary OO′. The channel surfaces are assumed to be diffuse with a tangential momentum accommodation coefficient

$$\sigma_t = \frac{u_r - u_i}{u_s - u_i}, \tag{11}$$

Table 1
Flow conditions and computational parameters[a]

Case:	Pong et al. [1]	Shih et al. [5]	Arkilic et al. [6]	Arkilic [7]
Gas:	N_2	He	Ar	He
Height (μm)	1.2	1.2	1.33	1.33
Width (μm)	40	40	52.3	52.3
Length (μm)	3000	4000	7490	7490
p_o (Pa)	1.01×10^5	1.00×10^5	1.01×10^5	6.5×10^3
Kn_o	0.05	0.135	0.05	2.0
σ_t	1.0	1.0	0.8	0.85
Cells	300×15	400×15	700×30	700×15
Sub-cells in each cell	5×2	5×2	5×2	5×2

[a] Gas and channel surfaces are assumed to have a temperature of 294 K to be consistent with all these experiments that were carried out at room temperature.

where u_i is the mean stream-wise velocity of incident molecules, u_r is the mean reflected stream-wise velocity and u_s is the surface stream-wise velocity. The value of σ_t, ranging between 0 and 1, depends upon the surface roughness and gas properties.

Arkilic et al. [6,7] developed a modified accumulation technique to measure low mass flux through micro-channels. Comparing the measured mass flow rate with the slip Navier–Stokes solution, they extracted σ_t for the micro-channel surfaces of single-crystal silicon in their system. The values appeared to range between 0.8 and 0.9, e.g., 0.80 ± 0.01 for argon and 0.88 ± 0.01 for nitrogen.

The same means was also utilized by Shih et al. [5] to extract σ_t for their micro-channel surfaces, yielding 0.9905 for nitrogen and 1.1620 for helium. However, the latter is beyond the physically realistic range of σ_t. It is known that the slip Navier–Stokes solution is no longer accurate beyond the slip regime as $Kn > 0.1$. In the helium experiment [5], the Knudsen number increased from 0.1 at the inlet to 0.16 at the outlet, where the extraction of σ_t through the slip Navier–Stokes solution became improper. In contrast, the Knudsen number in the nitrogen experiment [5] ranged between 0.025 and 0.05 that indicated the flow in the slip regime, which arrived at a reasonable value of σ_t, 0.9905. This demonstrated that the micro-channel surfaces in the UCLA system was close to the full diffusive reflection. The values of σ_t used in simulation are also listed in Table 1.

4. Results and discussion

4.1. Experimental micro-channels

In the first generation of experimental system for micro-channel gas flows developed by Pong et al. [1], six micro-pressure sensor holes were fabricated directly on the channel surfaces. Five inlet pressures of 5, 10, 15, 20 and 25 psig were employed, respectively, while the outlet pressure maintained at 1 atm. Fig. 6 compares the stream-wise pressure distributions given by the IP method with experimental data of Pong et al. [1], with the error bars to shown the measured confidence limits. The simulated and experimental results agree well with each other. Because of the small height of 1.2 μm, the velocity gradient in the normal direction is quite large that leads to a strong viscous effect and a rapid loss of pressure in the stream-wise direction. The viscous effect is clearly demonstrated by the non-linearity of the pressure profiles that

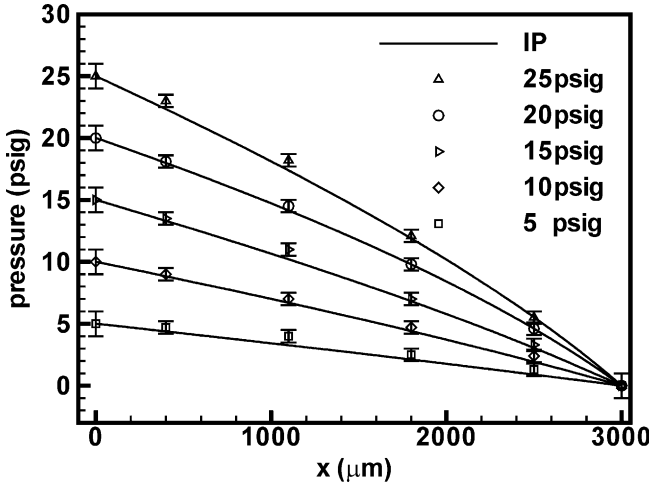

Fig. 6. Comparison of stream-wise pressure distributions given by IP with data measured by Pong et al. [1].

becomes significant as the inlet pressure increases. The pressure loss is subject to the local shear stress of the micro-channel surfaces that becomes sensitive to the Knudsen number as $Kn > 0.01$ [12]. For the same outlet pressure, the increase of the inlet pressure results in a more significant stream-wise variation of Kn. and therefore corresponds to a more obvious non-linear pressure profile.

In the second generation of experimental micro-channel system [5], 11 micro-pressure sensors were uniformly distributed along the channel surfaces of 4000 μm long. Two sensors were located at the entrance and the exit of the channel of 4800 μm long but not used in Fig. 8. In Fig. 7, the simulated mass flux by the IP method at the entrance pressures of 9.5, 15, 20 psig (different from inlet pressure 8.7, 13.6, 19 psig shown in Fig. 8), respectively, is compared against measured data of Shih et al. [5]. As one can see, there is a

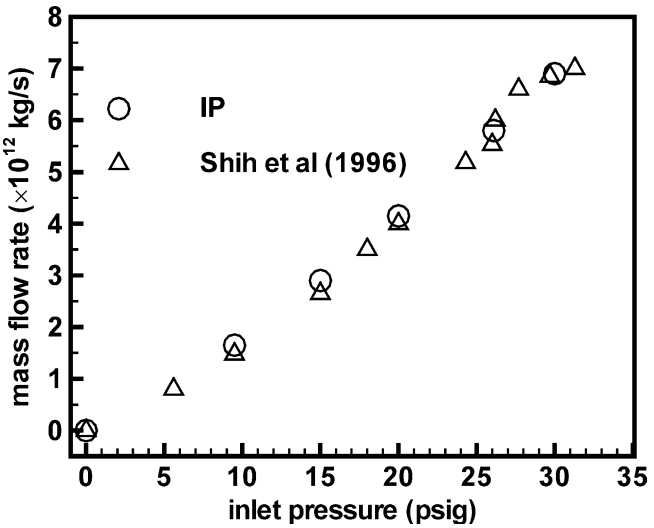

Fig. 7. Relation of mass flux versus the inlet pressure in the slip and transition regimes. Comparison of the IP simulation with the experimental data of Shih et al. [5].

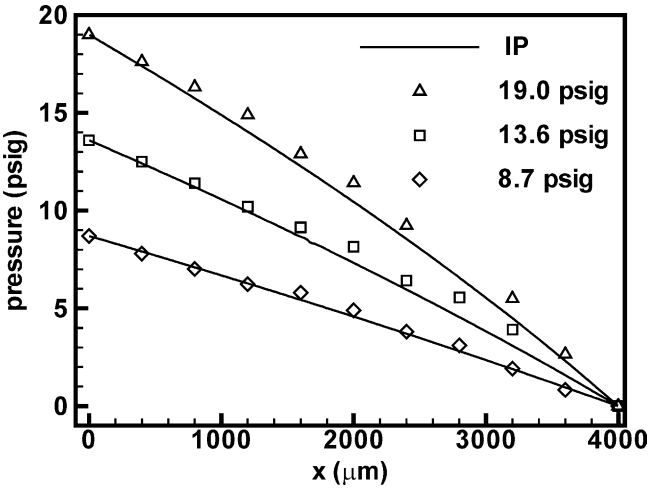

Fig. 8. Comparison of stream-wise pressure distributions given by IP with data measured by Shih et al. [5].

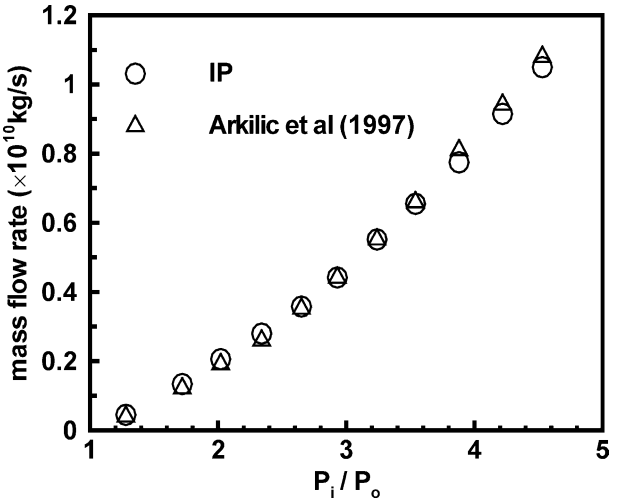

Fig. 9. Variation of mass flux versus the ratio of the inlet to outlet pressure in the slip regime. Comparison of the IP simulation with the experimental data of Arkilic et al. [6].

remarkable agreement. Fig. 8 shows the stream-wise pressure distributions at three different inlet pressures given by IP and experiment, which also agree with each other.

Because the height is of the order of micron, mass flux through micro-channels is as low as 10^{-12} kg/s. Arkilic et al. [6,7] developed a modified accumulation technique to measure such a low mass flux accurately. Fig. 9 compares the mass flow rates of nitrogen at an outlet Knudsen number of 0.05 given by IP calculations and Arkilic et al. experiment [6]. The flows were in the slip regime, and a remarkable agreement can be seen. Arkilic [7] also investigated flows in the transition regime. The inlet pressures of helium ranged between 133 and 413 kPa, corresponding to an inlet Knudsen number, Kn_i between 0.117 and 0.04, while the outlet exhausted to a low pressure of 6.5 kPa that gave rise to an outlet Knudsen number of 2.5. Therefore, a significant portion of the channel lay well beyond the slip flow regime. The slope of the measured flow conductance was approximately 11% greater than the slip Navier–Stokes prediction over the entire inlet pressure range [7]. The IP method is utilized to investigate this issue. The flow conductance as a function of mean pressure, $\overline{P} = (P_i + P_o)/2$ is shown in Fig. 10. The IP and measured results, except at the largest mean pressure where a difference of about 5% appears, are generally in good agreement.

4.2. Short micro-channels

In addition to various experimental conditions, a two-dimensional short micro-channel is investigated over the entire Knudsen regime from continuum to free molecular using the IP and DSMC methods. The micro-channel is 1 μm high and 15 μm long, and the surfaces are assumed to be fully diffuse. The pressure difference between the inlet and outlet leads to a stream-wise velocity at order of 10 m/s, this large velocity and the short length of the channel makes DSMC calculations affordable.

Fig. 11 shows the pressure and stream-wise velocity profiles of this short channel given by IP, DSMC, and the Navier–Stokes equation with a velocity-slip boundary condition. The inlet and outlet pressures are 1.2×10^5 and 1.0×10^5 Pa, respectively, which corresponds to a typical slip flow with Kn from 0.04 to 0.05. The three results agree well with each other. A sample size of 5×10^6 is used in the DSMC calculation to reduce statistical noise, 200 times larger than that used in the IP calculation.

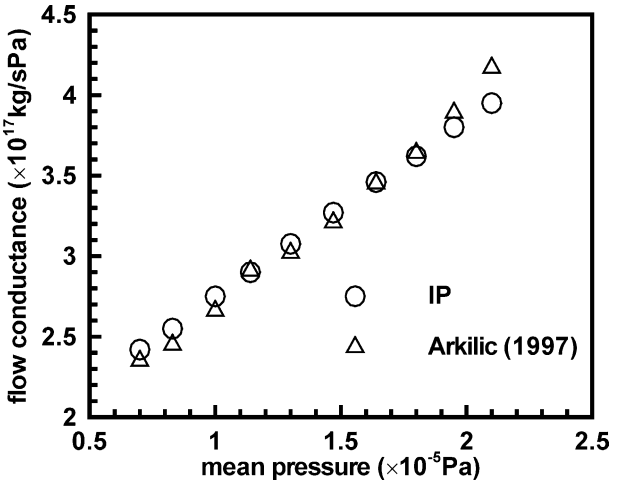

Fig. 10. Relation of flow conductance to mean pressure in the transition regime. Comparison of the IP simulation with the experimental data of Arkilic et al. [6].

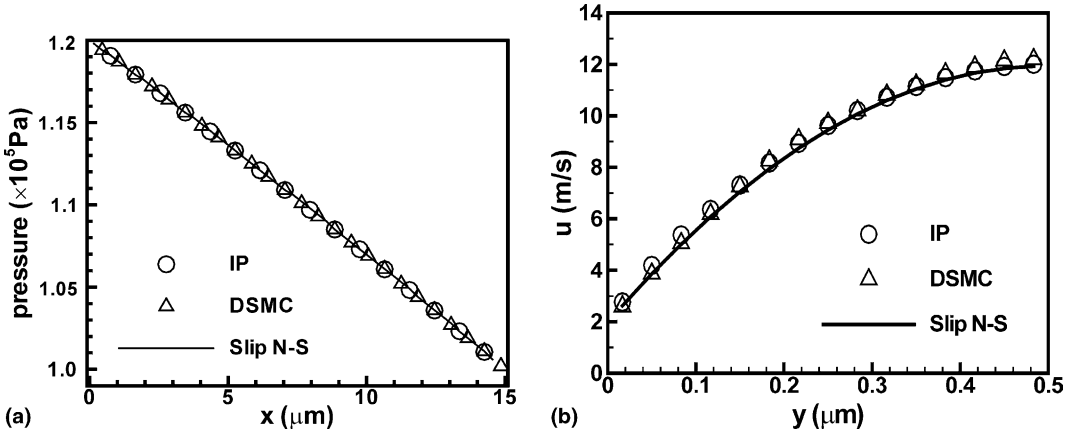

Fig. 11. Comparison of IP, DSMC and slip Navier–Stokes calculations for a short micro-channel flow in the slip regime. (a) Pressure distribution along the channel; (b) stream-wise velocity profile at a cross-section $x = L/2$.

Fig. 12 shows the evolution of stream-wise velocities in a cell located at the inlet center given by the IP and DSMC methods through statistically averaging the information velocities and the DSMC velocities of simulated molecules within the cell each time step, respectively. The mean number of simulated molecules is 50 each cell. Both of them start from a stationary flow field, simulated molecules are accelerated by the inlet and outlet pressure difference until a local balance between the pressure gradient and the surface shear stress is attained everywhere. As one can see, the stream-wise velocity given by IP evolves and statistically converges to a steady value of about 11 m/s after 180 time steps (Fig. 12(a)), while that given by DSMC submerges in statistical noise and fluctuates between 0 and 23 m/s (Fig. 12(b)). Therefore, it is seen, from this not too slow a flow in rather a short channel where DSMC works, that the IP method is preferable for low Mach number flows with boundary conditions that need to be determined by iteration.

The normalized mass flow rates as functions of the Knudsen number at the inlet, Kn_i are shown in Fig. 13, where the ratio of the outlet to inlet pressure is 0.7, the normalized factor of mass flux is $(\rho_i + \rho_o)v_m H/2$,

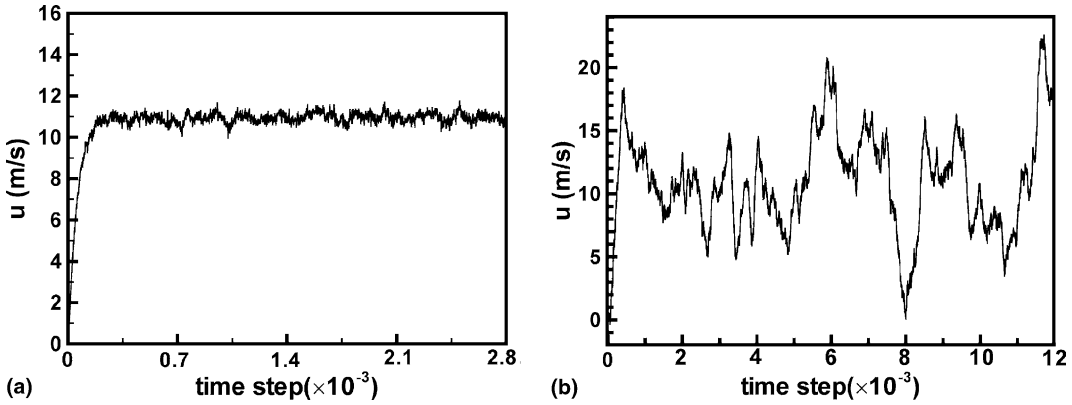

Fig. 12. Stream-wise velocities at the inlet center versus time steps given by statistically averaging the information velocity (a), and the velocity of the simulated molecules in DSMC (b).

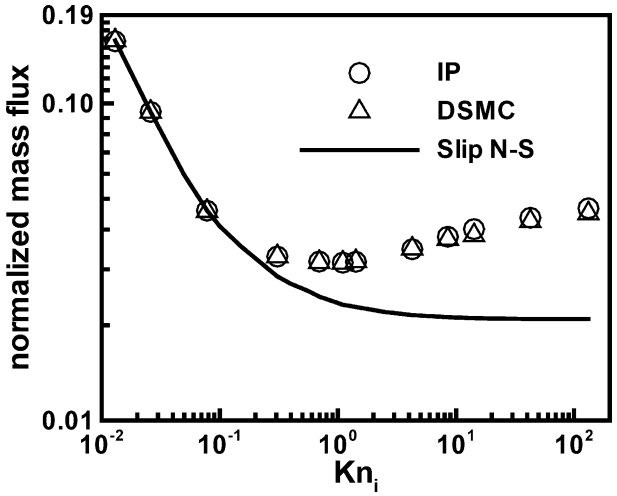

Fig. 13. Relation of the normalized mass flux versus the inlet Knudsen number (Kn_i) for a short micro-channel calculated by IP, DSMC and slip N–S methods.

ρ_i and ρ_o are the inlet and outlet densities, respectively, and $v_m = \sqrt{2RT}$ is the most probable thermal speed. The IP and DSMC results are in excellent agreement over the entire Knudsen regime, and demonstrate a minimum around Kn_i of 1. This phenomenon was first observed in experiment by Knudsen [26], and therefore is referred to as the Knudsen minimum. The slip Navier–Stokes solution accords with the IP and DSMC results in the slip regime as $Kn_i < 0.1$, but deviates from them in the transition regime and fails to predict the Knudsen minimum.

5. Conclusions

In simulating the large length to height ratio and slow micro-channel gas flows under experimental conditions one encounters the problem of big noise to useful information ratio and difficulty in regulating

the boundary conditions at the inlet and outlet. The needs of DSMC method in the huge sample size and extremely large computation time made its simulation of such flows beyond the current computer capacities. In the present paper the low speed flows in long micro-channel were simulated using the IP method. A conservative scheme for the IP values to guarantee the adjustment of the inlet and outlet boundary conditions and a super-relaxation technique to speed up the convergent process of IP calculations were employed. These have the universal significance in simulating all low speed micro-scale internal flows. The stream-wise pressure profiles and mass fluxes given by the IP method agree well with the measured data available [1,5–7] which show the efficiency of the method employed.

Short and not too slow micro-channel gas flows over the entire flow regime from continuum to free molecular was investigated using the IP and DSMC methods. In the slip regime, the velocity and pressure profiles given by the IP and DSMC methods and the Navier–Stokes equations with a slip boundary condition agreed well with each other. However, the slip Navier–Stokes mass flux significantly deviated from the two others when the Knudsen number was greater than 0.1, and could not predict the famous Knudsen minimum observed in experiment [13,26] and in the present IP and DSMC calculations. This indicated that the means to extract the tangential momentum accommodation coefficient of micro-channel surfaces from measured mass flux in comparison with the slip Navier–Stokes solution is appropriate only when experiment was carried out in the slip or continuum regime.

Acknowledgements

The support of the National Natural Science Foundation of China (Grants 19889209, 90205024) is sincerely appreciated.

References

[1] K.C. Pong, C.M. Ho, J.Q. Liu, Y.C. Tai, Non-linear pressure distribution in uniform micro-channels, ASME-FED 197 (1994) 51.
[2] E.B. Arkilic, K. Breuer, M.A. Schmidt, Gaseous slip flow in long micro-channels, J. MicroElectroMech. Syst. 6 (1995) 167.
[3] J.C. Harley, Y. Huang, H. Bau, J.N. Zemel, Gas flow in micro-channels, J. Fluid Mech. 248 (1995) 257.
[4] J.C. Shih, C.M. Ho, J. Liu, Y.C. Tai, Non-linear pressure distribution in uniform microchannels, ASME-AMD 238 (1995).
[5] J.C. Shih, C.M. Ho, J.Q. Liu, Y.C. Tai, Monatomic and polyatomic gas flow through uniform microchannels, ASME-DSC 59 (1996) 197.
[6] E.B. Arkilic, M.A. Schmidt, K.S. Breuer, Measurement of the TMAC in silicon microchannels, in: C. Shen (Ed.), Rarefied Gas Dynamics, Peking University Press, 1997, p. 983.
[7] E.B. Arkilic, Measurement of the mass flow and tangential momentum accommodation coefficient in silicon microchannels, Ph.D. thesis, MIT, FDRL TR 97-1, 1997.
[8] C.M. Ho, C.Y. Tai, Micro-electro-mechanical-systems (MEMS) and fluid flows, Ann. Rev. Fluid Mech. 30 (1998) 579.
[9] A. Beskok, G. Karniadakis, Rarefaction and compressibility effects in gas microflows, J. Fluids Eng. 11 (1996) 448.
[10] E.S. Oran, C.K. Oh, B.Z. Cybyk, Direct simulation Monte Carlo: recent advances and applications, Ann. Rev. Fluid Mech. 30 (1998) 403.
[11] J. Fan, C. Shen, Statistical simulation of low-speed unidirectional flows in transitional regime, in: R. Brun, R. Campargue, R. Gatignol, J.C. Lengrand (Eds.), Rarefied Gas Dynamics, Cepadues Editions, vol. 2, 1999, p. 245.
[12] J. Fan, C. Shen, Statistical simulation of low-speed rarefied gas flows, J. Comput. Phys. 167 (2001) 393.
[13] W. Dong, University of California Report UCRL-3353, 1956.
[14] T. Ohwada, Y. Sone, K. Aoki, Numerical analysis of the Poiseuille flow and thermal transpiration flows between two parallel plates on the basis of the linearized Boltzmann equation for hard-sphere molecules, Phys. Fluids 1 (1989) 2042.
[15] Y. Sone, S. Takata, T. Ohwada, Numerical analysis of the plane Couette flow of a rarefied gas on the basis of the linearized Boltzmann equation for hard-sphere molecules, Eur J. Mech. B/Fluids 9 (1990) 273.
[16] Q. Sun, I.D. Boyd, G.V. Cadnler, Numerical simulation of gas flow over micro-scale airfoils, AIAA 2001-3071, 2001.
[17] S.A. Schaff, F.S. Sherman, Skinfriction in slip flow, J. Aero. Sci. 21 (1954) 85.
[18] Z. Janour, Resistances of a plate in parallel flow at low Reynolds numbers, NACA TM 1316 (1954).

[19] C.P. Cai, I.D. Boyd, J. Fan, G. Candler, Direct simulation methods for low-speed microchannel flows, J. Thermophys. Heat Transf. 14 (2000) 368.
[20] C. Xie, J. Fan, C. Shen, Statistical simulation of micro-channel gas flows, in: Proceedings of Mass and Heat Transfer of Chinese Society of Engineering Thermophysics, 2000, pp. 388–390 (in Chinese).
[21] G.A. Bird, Molecular Gas Dynamics and the Direct Simulation of Gas Flow, Clarendon Press, 1994.
[22] J. Fan, I.D. Boyd, C.P. Cai, K. Hennighausen, G.V. Candler, Computation of rarefied gas flows around a NACA 0012 airfoil, AIAA J. 39 (2001) 618–626.
[23] C. Shen, J.Z. Jiang, J. Fan, Information preservation method for the case of temperature variation, in: T.J. Bartel, M.A. Gallis (Eds.), Rarefied Gas Dynamics, 185, AIP, 2001.
[24] C. Shen, Rarefied Gas Dynamics, National Defense Industry Press, Beijing, 2003 (in Chinese).
[25] R.P. Nance, D. Hash, H.A. Hassan, Role of boundary conditions in Monte Carlo simulation of MEMS devices, J. Thermophys. Heat Transf. 11 (1997) 497.
[26] M. Knudsen, Ann. Phys. 28 (1909) 75.